# NOTES AND CORRESPONDENCE

## On the Effects of Islands' Geometry and Size on Inducing Sea Breeze Circulation

Y. MAHRER[1]

*Cooperative Institute for Research in the Atmosphere, Colorado State University, Fort Collins, CO 80523*

M. SEGAL

*Department of Atmospheric Science, Colorado State University, Fort Collins, CO 80523*

25 April 1984 and 21 September 1984

ABSTRACT

Model scaling of the characteristics of the sea breeze circulation involved with circular and slab elongated-symmetric midlatitude islands was performed. Larger horizontal and vertical velocities were indicated over the small circular islands as compared to those over corresponding elongated islands. The circulation characteristics of both types of islands become similar when the half-width of the island is about the same as the distance of inland penetration of the sea breeze in a nonisland case. Evaluation of the results through a scale analysis is presented.

### 1. Introduction

Under light synoptic flow, the sea breeze (SB) circulation may be an important atmospheric process over islands during the warm season. It is expected that the size and geometry of islands play an important role in the determination of their SB characteristics as reflected by 1) the SB flow intensities and 2) the peak values of the vertical velocities.

Some attention has been given in the literature to the properties of midlatitude SB circulation in those cases; however, only a partial examination has been made. The modeling study by Neumann and Mahrer (1974), for example, was limited to the evaluation of a SB of a small circular island (radius of 26.25 km) and a large one (radius of 51.25 km). Recently, Abe and Yoshida (1982) evaluated by modeling means the SB characteristics as a function of the size of elongated slab symmetric islands.

It is the purpose of the current Note to provide some complementary insight into previous studies by comparing the SB characteristics of both types of islands. A series of numerical model simulations were carried out to obtain the required data. In addition, scale analysis is performed for further interpretation of the results. For each type of island the SB flow intensity and peak values of vertical velocity are examined, and their asymptotic trend as the size of the island increases is investigated. Emphasis has been given to comparison of these characteristics for both types of islands.

### 2. Numerical model aspects

The formulation of the model adopted in the present study is given in Neumann and Mahrer (1971, 1974); the input data were also adapted from these studies. However, the model formulation of Neumann and Mahrer (1971) was modified for the case of elongated island simulations to follow the constraints used in Neumann and Mahrer (1974) at the center of the circular islands. In consideration of the expected development of strong vertical velocities in the current study, this model has the advantage of being nonhydrostatic, while it also has the option for both Cartesian and cylindrical coordinate systems. In addition, it is computationally relatively inexpensive as applied to the refined temporal and spatial scales in this set of simulations.

The simulations performed in this study consist of a 12 hour integration, beginning at 0800 LST for summer conditions in the Eastern Mediterranean (latitude 32°N). The simulations were performed for circular islands with radii of 5, 10, 20, 30, 40, 60 and 80 km. Similar simulations were carried out for symmetrical infinite elongated islands with the same half-width. It is worth stressing that the physical constraints involved with elongated and circular islands justify (in the absence of synoptic flow) using two-dimensional slab-symmetric and axisymmetric models. The numerical and physical formulations used for both types of islands are the same. A simulation for a nonisland case (namely, a straight

[1] On sabbatical leave from The Hebrew University of Jerusalem, Seagram Centre for Soil and Water Science, Faculty of Agriculture, Rehovot, 76100 Israel.

shore line dividing sea and land domains) is also included for comparison.

In order to ensure adequate resolution of the SB frontal region a relatively small horizontal grid interval of 1 km was adopted. The simulated domains consist of a sea section of 40 km in all cases (we found this size of water domain to be sufficiently large to resolve the SB circulation for the variety of island sizes in this study). In the vertical, a constant grid resolution of 100 m above the surface layer was adopted. The model top was set at 3 km, based on preliminary simulations indicating that an additional increase of the top height provided no advantage in further refinement in the features of relevance in the current study. The integration time interval was 15 s.

## 3. Results

The results illustrate the time dependence of the maximum wind speed at a height of 25 m ($U_{max}$) along the domain cross section, for various island sizes, as well as the maximum vertical velocity ($W_{max}$) in the computational domain. It is worth noting that $U_{max}$ and $W_{max}$ were obtained either in the vicinity of the SB front, or near the island center following the arrival of the SB front at that location.

Figure 1a presents $U_{max}$ for the elongated islands. Over small islands, convergence of the SB at the center occurs relatively early; after convergence occurs, $U_{max}$ is relatively constant. Peak values of $U_{max}$ increase with the size of the islands while their duration is shortened. In our case, an island of 80 km half-width produced similar results to those obtained in the non-island case, indicating that the inland penetration of the SB is of about the same distance.

In the circular islands (Fig. 1b), $U_{max}$ reached higher peak values than in the corresponding elongated islands. For the 5 km island, the peak value was about 0.5 m s$^{-1}$ higher, while for the 20 km island it was 2.7 m s$^{-1}$ higher. For the 10, 20, and 30 km islands, the first peak values were found to coincide with the convergence of the SB front at the center of the island. As the island size increases, the behavior of $U_{max}$ tends to be similar to that predicted over a similarly-sized elongated island (since the shore curvature for both types tends to become identical).

The patterns of $W_{max}$ in the computational domain are given in Fig. 2a (elongated islands) and in Fig. 2b (circular islands). The peak values of $W_{max}$ are attributed to: 1) convergence of the opposing SB fronts in the vicinity of the island center, 2) intensification of the SB front toward noon, and 3) secondary intensification of the SB in the afternoon hours (e.g., Neumann and Mahrer, 1971; Simpson *et al.*, 1977). The peak values of $W_{max}$ for the circular islands of radii 5 and 10 km are significantly higher for several hours than those over the corresponding elongated islands because of the convergence effect which occurs relatively early in the morning. As the island size is increased to within the range of the daily inland penetration of the SB front, both island types reveal similar patterns of $W_{max}$, with their structure tending to coincide with the non-island case. The convergence of the flow in the vicinity of the island center is very noticeable in the circular island, as indicated by the temporary sharp increase of $W_{max}$ (noted by c in Fig. 2b). The sharp increases of the vertical velocity within a short time interval indicate the possible advantage in using a nonhydrostatic model for the simulations. These sharp increases in $W_{max}$ are not diagnosed in the elongated island simulations.

## 4. Analysis

### *a. Mesoscale available potential energy evaluations*

The greater wind speed which is predicted for the small circular islands as compared to equivalent

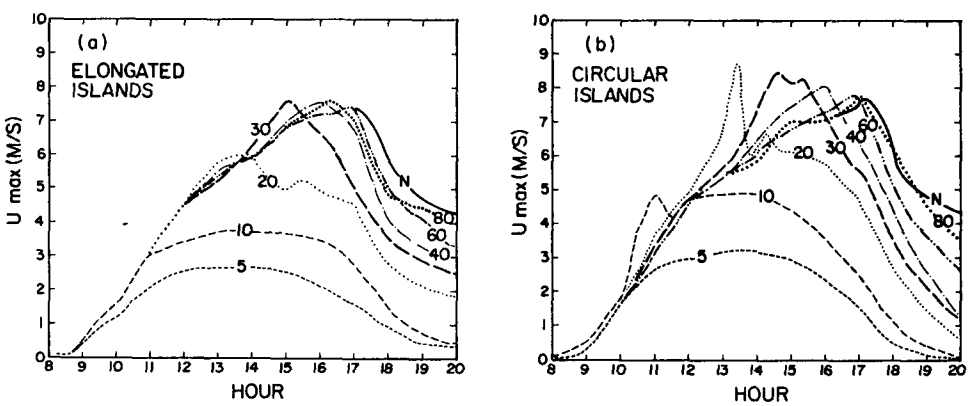


FIG. 1. Maximum wind speed ($u_{max}$) at a height of 25 m along the domain cross section as a function of time for (a) elongated symmetric islands (half-width indicated in km) and (b) circular islands (radii indicated in km); *N* indicates the nonisland case.

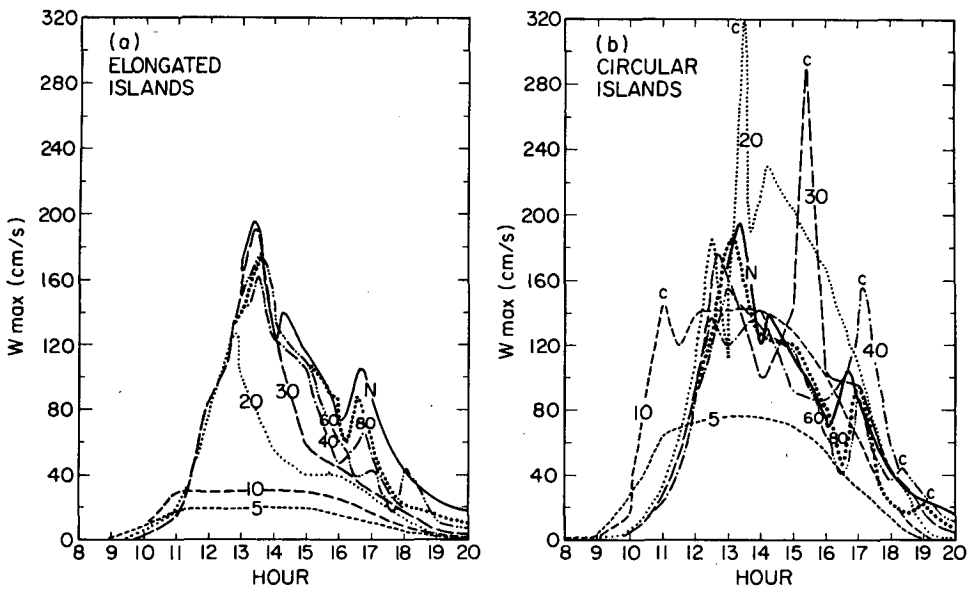


FIG. 2. Maximum vertical velocity in the computational domain cross section for (a) elongated symmetric islands (half-width indicated in km) and (b) circular islands (radii indicated in km); *N* indicates the nonisland case.

elongated islands, when the SB front approaches the island center, is examined; i.e., by using the Mesoscale Available Potential Energy (MAPE) formulation as suggested by Green and Dalu (1980). The kinetic energy of the SB circulation relates to the amount of MAPE. Hence, comparing the MAPE involved with the two island types provides an indication of the relative wind speeds involved with the two cases. Adopting the Green and Dalu approach, we note that the $\mathrm{MAPE_L}$ (for elongated islands) and $\mathrm{MAPE_C}$ (for circular islands) per unit area are given as

$$\mathrm{MAPE_L} = K(d - a_L)\left(1 - \frac{d - a_L}{D + e - a_L}\right)\Big/ (D + e - a_L), \quad (1)$$

$$\mathrm{MAPE_C} = K(d^2 - a_C^2)\left(1 - \frac{d^2 - a^2}{D^2 - a_C^2}\right)\Big/ (D^2 - a_C^2), \quad (2)$$

where $K$ is a scaling factor, $d$ the half-width (or radius) of the island, $(D - a_C)$ the length of the section in which the SB circulation exists for the circular island (see Fig. 3). For the elongated islands the offshore extent of the SB system is considered to be different by $e$ from that involved with circular islands (namely, the SB system is of horizontal scale of $D - a_L + e$, the simulation results indicated that, as expected, $e \geq 0$; e.g., see Fig. 5). In order to simplify our analysis, it will be applied to a situation in which $a_L = a_C = 0$, namely, when the SB system occupies the whole inland region of the islands.

Assuming the same efficiency transfer of the MAPE to kinetic energy in both island types, one obtains the following ratio for the typical squared wind speeds.

$$R = \frac{U_C^2}{U_L^2} = \frac{[(D^2/d^2) - 1][(D/d) + (e/d)]^2}{D^4/d^4[(D/d) + (e/d) - 1]}. \quad (3)$$

In order to evaluate $R$ we constructed a nomogram describing $R$ as a function of $D/d$ and $e/d$. The nomogram (Fig. 4) indicates that roughly $R \approx 1$ for reasonably feasible values of these parameters. Quantitative determination of $D/d$ and $e/d$ is largely subjective. However, generally for the islands with radii smaller than 30 km we estimate from the simulated fields that these parameters can be constrained by $(D/d) \geq 1.5$ and $(e/d) \geq 0.5$, following the convergence at the island's center. Examination of the nomogram indicates that with this estimation it is likely that $R \geq 1$ for those islands, as long as $(D/d) \approx 1.5$ (occurring around the convergence time). Toward the evening the offshore penetration of the circulation results in some increase of $D/d$ which is larger than that involved with $e/d$; hence by then it is likely that $R \leq 1$. Indeed, examining the patterns of $U_{max}$ for

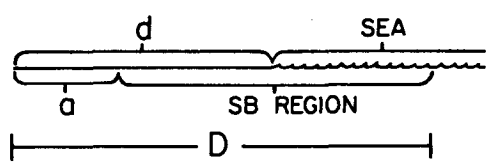


FIG. 3. Schematic of pertinent horizontal scales involved with the sea breeze circulation of islands.

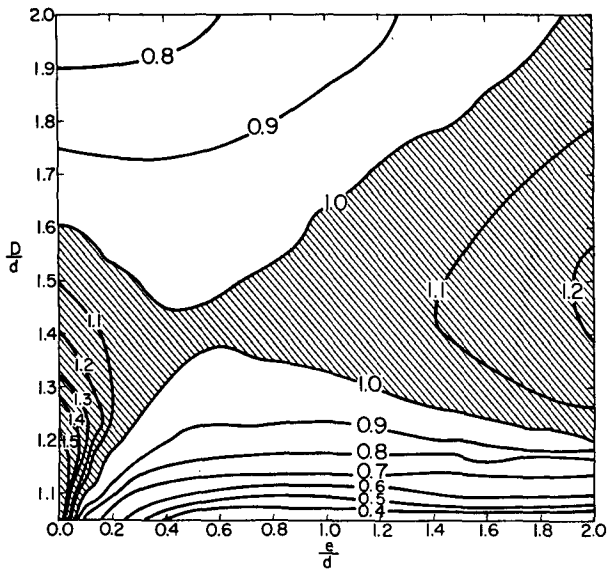


FIG. 4. Nomogram evaluating $U_C^2/U_L^2$ following a convergence of the sea breeze at the island center (see text for symbols).

both types of islands in the afternoon hours reveals somewhat stronger $U_{max}$ for the elongated group.

To illustrate the horizontal scales involved with the SB system in both types, we selected the 20 km islands, in which the development is significantly pronounced. The horizontal extent of the SB system can be indicated by the intensity of the cross-shore wind component. Figure 5 illustrates a vertical cross section of the cross-shore wind component at 1300 LST (just before the convergence of SB in the center of the islands). Stronger onshore flow and return flow aloft are predicted for the circular island. However, the horizontal extent of the system is larger in the elongated island.

*b. Mass conservation considerations*

Scaling the SB characteristics by using the continuity equation should also be considered in our analysis. From the continuity equation, we have for circular islands

$$W(z) = -\int_0^z [(\partial u/\partial r) + (u/r)]dz, \qquad (4)$$

where $u$ is the radial component of the wind, $r$ the distance from the center of the island and $z$ the height.

For radial flows, in the absence of a vertical component of velocity ($W(z) = 0$), Eq. (4) suggests that the intensity of $u$ is proportional to $1/r$. Obviously, however, the SB circulation of circular islands, include nonzero vertical velocities. Hence, mass conservation should be achieved through the enhancement of both vertical and radial components of velocity. Results of the simulations indicated that for scaling purposes $(\partial u/\partial r)_C \geq (\partial u/\partial x)_L$. If we assume an extreme situation in which $(\partial u/\partial r)_C \approx (\partial u/\partial x)_L$, the term $u/r$ will provide additional enhancement of $W$ in the circular islands as compared to the elongated islands. In this situation, when the flow is converging at the islands center, choosing typical scales of $z = 1000$ m, $u = 3$ m s$^{-1}$ and $r = 3000$ m in relation to the simulations of the 5 and 10 km islands, results in $W_C = W_L + 1$ m s$^{-1}$. Based on Fig. 2 such a magnitude enhancement of the vertical velocities over circular islands as compared to elongated ones is typical. For the 20 km islands (Fig. 5), representative values at a distance of 3 km from their center are $u = 3$ m s$^{-1}$ and $z = 2000$ m. According to the analysis, this implies a difference of 2 m s$^{-1}$ in $W_{max}$ by the time of flow convergence at the center of the islands.

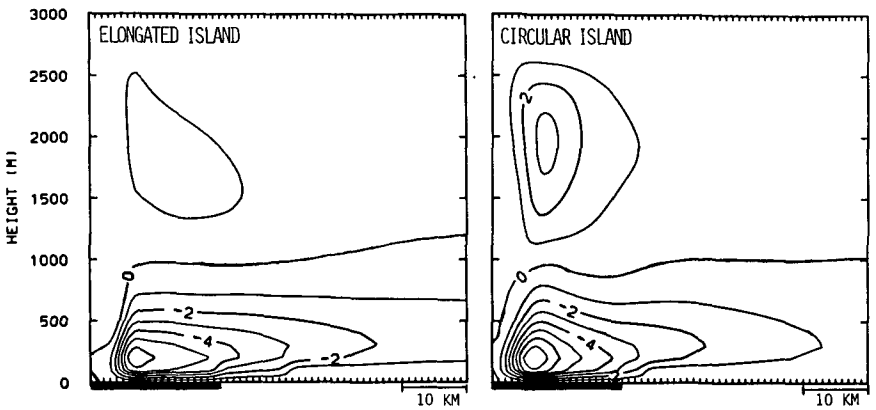


FIG. 5. Vertical cross section of the cross-shore wind component (in m s$^{-1}$) for the 20 km islands at 1300 LST (dark contours indicate return flow). The islands half-width is shown by dark lines (bottom).

## 5. Conclusions

The current study indicates the important role that island size and geometry play in the determination of some SB circulation characteristics. It is suggested that these characteristics will also be partially obtained for irregular curved islands or peninsula instead of the ideal circular or elongated islands (e.g., Pielke, 1974). An absence of synoptic flow was assumed in the present study in order to enable simple, inexpensive preliminary modeling evaluations, as well as to perform scale analysis. When synoptic flow exists, the predicted patterns would be modified. These modifications, however, can be qualitatively evaluated from the knowledge that we have about the coupling of sea breezes with synoptic flows (e.g., Estoque, 1962; Pielke, 1974; Physick, 1976; Simpson *et al.*, 1977, among others). The most significant result is that circular islands with an appropriate size produce considerably stronger vertical velocities (in our simulations up to five times larger), than elongated islands of equal width. Hence, for example, under supportive atmospheric conditions, one can expect that cloud triggering will be the more pronounced over circular than over elongated islands with an equivalent width.

The scale analysis suggests that mass conservation in the small and medium circular islands is maintained by a significant intensification of the vertical velocities as the SB penetrates onshore, rather than by strong enhancement of the horizontal radial flow. The analysis also suggests higher density of MAPE for circular islands by the time the flow converges at the center. However, toward evening, elongated islands are likely to possess higher densities of MAPE. These trends in MAPE are reflected in the simulated values of $U_{max}$ for both island types.

*Acknowledgment.* Partial support for this study was provided by Grants ATM8304042 and ATM8414181 of the National Science Foundation and NASA Grant NAG-5-359. The model computations were carried out using the NCAR computer (NCAR is supported by the National Science Foundation). The authors thank R. Arritt, G. Dalu, R. Kessler, Y. Ookouchi and R. Pielke for useful discussions.

### REFERENCES

Abe, S., and T. Yoshida, 1982: The effect of the width of a peninsula on the sea breeze. *J. Meteor. Soc. Japan.*, **60,** 1074–1084.

Estoque, M. A., 1962: The sea breeze as a function of prevailing synoptic situation. *J. Atmos. Sci.*, **19,** 244–250.

Green, J. S. A., and G. A. Dalu, 1980: Mesoscale energy generated in the boundary layer. *Quart. J. Roy. Meteor. Soc.*, **106,** 721–726.

Neumann, J., and Y. Mahrer, 1971: A theoretical study of the land and sea breeze circulations. *J. Atmos. Sci.*, **28,** 532–542.

——, and Y. Mahrer, 1974: A theoretical study of the sea and land breezes of circular islands. *J. Atmos. Sci.*, **31,** 2027–2039.

Physick, W. L., 1976: A numerical model study of sea breeze phenomenon over lake of gulf. *J. Atmos. Sci.*, **33,** 2107–2135.

Pielke, R. A., 1974: A three dimensional numerical model of the sea breeze over south Florida. *Mon. Wea. Rev.*, **102,** 115–139.

Simpson, J. E., D. A. Mansfield, and J. R. Milford, 1977: Inland penetration of sea breeze fronts. *Quart. J. Roy. Meteor. Soc.*, **103,** 47–76.